IMPACT OF PARTICLE SIZE OF CAC ON ITS HYDRATES AT 40 °C

Xuejun Shang, Xuekun Tian, Yaxian Liu, Liugang Chen, Guotian Ye

Henan Key Laboratory of High Temperature Functional Ceramics, School of Materials Science and Engineering, Zhengzhou University, Zhengzhou, 450001 Henan, People's Republic of China

ABSTRACT

In this work, the effect of particle size of calcium aluminate cement (CAC) on its hydration products during hydration at 40 °C was studied. The cement hydration at the designated times was terminated by the freeze vacuum drying method. The phase development and microstructure evolution during the cement hydration were investigated by XRD and SEM, respectively. The dependence of quantity and the degree of crystallinity of C_3AH_6 on the reducing particle size of CAC after hydration at 40 °C is investigated and discussed.

INTRODUCTION

Calcium aluminate cement (CAC) is a hydraulic binder commonly used in castables[1]. It is known that the particle size of the cement influences the hydration behavior of the cement[2], and consequently affects the setting and hardening processes of castables[3]. Moreover, the temperature of castable placement environment may be different at different regions and in different seasons and CAC may have varied hydration behavior at different environmental temperatures[4].

It is known that curing temperature is one of the main parameters that affect the hydration rate and hydration products of the cement[5]. For example, $CaO{\cdot}Al_2O_3{\cdot}10H_2O$ (CAH_{10}) is the main hydrate at temperatures below 15 °C, whereas CAH_{10} and $2CaO{\cdot}Al_2O_3{\cdot}8H_2O$ (C_2AH_8) are formed at temperatures between 15 °C and 35 °C[6]. As CAH_{10} and C_2AH_8 compounds are thermodynamically metastable, they have a higher solubility than the stable phases of $3CaO{\cdot}Al_2O_3{\cdot}6H_2O$ (C_3AH_6) and $Al(OH)_3$ (AH_3)[7]. Once stable phases start to nucleate, the metastable phases dissolve, and further convert into C_3AH_6 with the curing time and temperature.

In our previous work[8], it has been found that the amount of CAH_{10} is lower with the prolonging grinding time of the cement after curing at 20 °C for 18h, indicating that the hydration rate of cement at 20 °C is decreased with the decreasing cement particle size. However, little information exists about the hydration rate of CAC with reduced sizes at 40 °C. In this work, commercial calcium aluminate cement was ground with various times to obtain cement samples with different particle sizes. The hydration behavior of the cement pastes and mortars were determined by exothermic reaction. The hydration of the cement pastes was halted by freeze vacuum drying method after curing for the designated times and dried samples were analyzed by XRD and examined by SEM.

EXPERIMENTAL PROCEDURES

Commercial calcium aluminate cement was used in this work. The major chemical composition and mineralogical composition of the cement are listed in Table 1.

Tab. 1: Major chemical and mineralogical composition of CAC (wt %).

CaO	Al_2O_3	CA	CA_2	$C_{12}A_7$	α-Al_2O_3
24.91	73.97	57.76	16.15	0.16	23.83

The cement was dry ground for one hour and two hours, respectively, to decrease the particle sizes. For each batch, 5 kg of the commercial cement was fed into a laboratory mill (500 mm in length and 500 mm in diameter). A combination of 100 kg cylindrical steel rods and spherical steel balls was used as the grinding media with a cement/grinding media weight ratio of 1/20.

Hydration heat evolution curves of CAC pastes were detected by a semi-adiabatic method at 40 °C. The water/cement ratio of the cement pastes was 0.3. The thermocouple was embedded in the paste sample, and the curve of temperature vs. time was recorded by a computer.

The as-prepared cement pastes after curing for a predetermined time at 40 °C were frozen at -40 °C to halt the hydration and then dried under vacuum at 60 Pa at 20 °C. The phase compositions and morphology of the dried cement pastes were characterized by XRD (D8 Focus, Bruker, Germany) and SEM (ZEISS-FESEM MERLIN Compact, Germany), respectively.

RESULTS AND DISCUSSION

The particle size distributions of the cements with and without grinding are shown in Fig. 1. The particle fraction of larger than 30 μm is 20 % for the cement without grinding. In comparison, the particle fraction of larger than 30 μm disappears for the cements after grinding for 1h and 2h. Meanwhile, the particle fraction of smaller than 3 μm is 16 % for the cement without grinding, while this fraction is 45 % for the cement after grinding for 1h and 94 % for the cement after grinding for 2h. Therefore, the above results indicate that the particle size of the cement is considerably reduced with the grinding time.

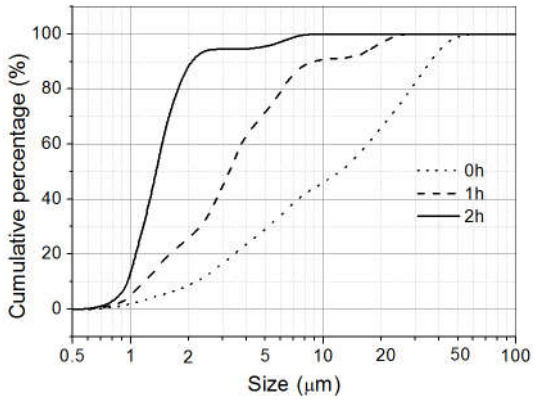

Fig. 1: Cumulative distribution of the cements after grinding for 0h, 1h and 2h.

The hydration heat curves of cement pastes after grinding for 0h, 1h and 2h at 40 °C are shown in Fig. 2. It is seen from the figure that the sample without grinding has a dormant period of about 3.7h, while the samples after grinding for 1h and 2h have a dormant period of about 2.5h. It is also can be seen from Fig. 2 that the peak temperature of the sample without grinding appears at about 4 h of hydration, while those of the both samples after grinding for 1h and 2h appear for about 2.65h of hydration. The above results show that the dormant period is shortened and the time to peak temperature is reduced with the increasing grinding time. These results demonstrate that the hydration rate of the cement paste increases with the reducing particle size of the cement at 40 °C.

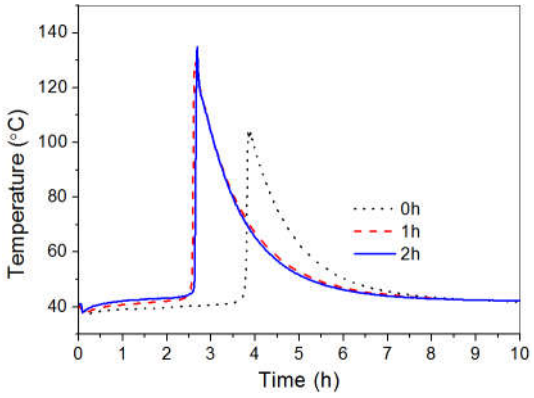

Fig. 2: Hydration heat curves of cement pastes at 40°C.

Figure 3 presents the XRD patterns of the samples of the cement pastes after grinding for 0h, 1h and 2h after curing at 40 °C for 3.5h. It is seen in Fig. 3 that hydrated products are not detected in the paste of CAC as received after 3.5h of hydration at 40 °C. In comparison, C_3AH_6 and AH_3 are the major hydrates in the ground cement pastes, and the peak height of C_3AH_6 at 17.27° increases with the grinding time, further confirming that the hydration rate of the cement paste and the amount of C_3AH_6 increase with the reducing particle size of the cement at 40 °C.

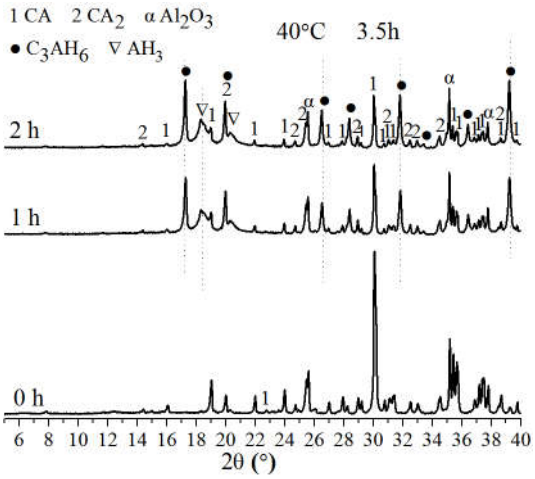

Fig. 3: XRD patterns of the pastes of CAC with grinding for 0h, 1h and 2h and hydration for 3.5h at 40°C.

Figure 4 shows the XRD patterns of pastes of the cement after grinding for 0h, 1h and 2h after curing at 40 °C for 6h. There is not noticeable difference in the

main hydrates of C_3AH_6 and AH_3 in the pastes of as-received and ground CAC after 6h of hydration at 40 °C. Compared with the unground cement, although grinding for 1h and 2h accelerated the hydrates formation (Fig. 3) during hydration, the grinding produced no obvious difference in the hydrates formation after a longer hydration period (Fig. 4).

Figure 5 is the microstructure of CAC pastes hydrated for 6h at 40 °C. It is can be seen in Figs. 5a-c that granular-shaped crystals of C_3AH_6 are found on the CAC particles in the cement pastes. The average crystal size of C_3AH_6 in Figs. 4a-c is 158 nm, 370 nm and 980 nm, respectively. It is interesting to mention that the crystal size of C_3AH_6 increases with the reducing particle size of the cement at 40 °C. These results indicate that the microstructure of the hydrated cement changes and the degree of crystallinity of C_3AH_6 increases with the reducing particle sizes of CAC at 40°C.

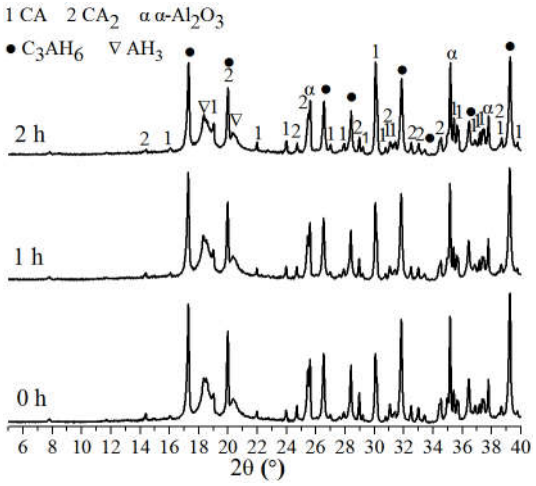

Fig. 4: XRD patterns of the pastes of CAC with grinding for 0h, 1h and 2h and hydration for 6h at 40°C.

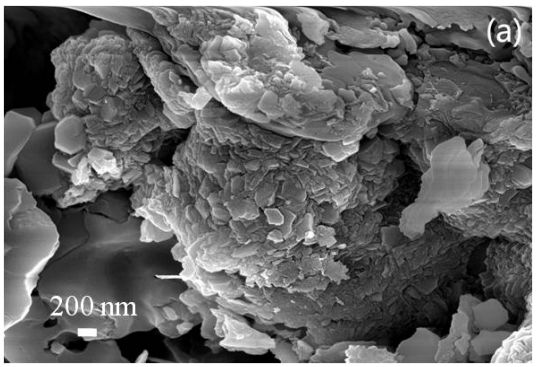

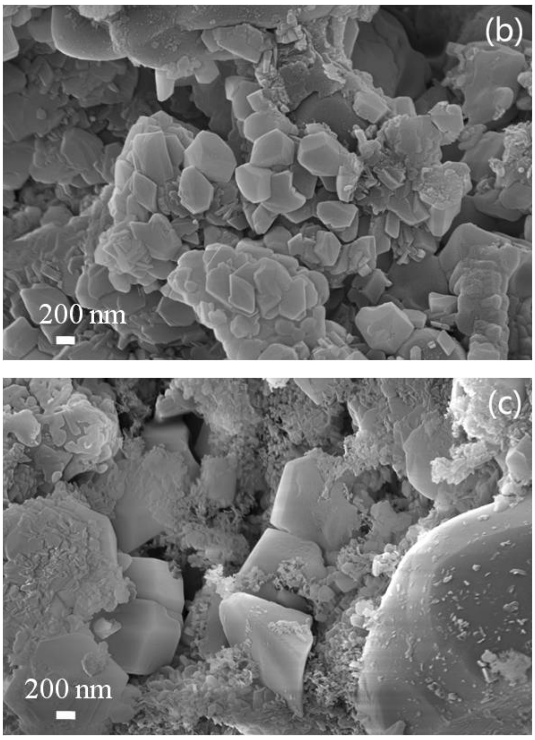

Fig. 5: SEM micrographs of the pastes of CAC with grinding for 0h (a), 1h (b) and 2h (c) and hydration for 6h at 40 °C.

As proposed in the reports[9,10], the stable crystalline hydrate at 40 °C was C_3AH_6 which precipitate near the surface of the cement and in the pores between the cement particles. As seen in the particle size distribution of the cement with and without grinding in Fig. 1, both coarse and fine particles present in the as-received cement. In comparison, the size fraction of 0.5-3 μm is increased at the expense of the coarse particles in the range of 10-50 μm, as a result, the cement after grinding only composed by fine particles. As shown in the schematic structures of the as-received cement (Fig. 6a), the pores among the coarse cement particles and fine particles are rare because of the dense agglomerate structure. The crystal size of C_3AH_6 which always precipitate in the pores cannot grow freely without sufficient space.

By contrast, it is seen in Fig. 6b that CAC particles after grinding for 1h and 2h are loosely accumulated with many pores in the structure as the particle size distribution concentrating to fine particles. So it is probably that the cubic C_3AH_6 forms freely during hydration, which is in contact with anhydrous phases and water. Therefore, the crystal size of C_3AH_6 is

growing with the reducing particle sizes of CAC at 40 °C. Moreover, C_3AH_6 can be produced only via conversion from C_2AH_8 according to the following reaction[9,10]:

$$C_2AH_8+CA+H\rightarrow C_3AH_6+AH_3 \quad (1)$$

This transformation is followed by substantial porosity generation associated with higher density of C_3AH_6 (2.52 g/cm^3) than C_2AH_8 (2.05 g/cm^3)[5], leading to the anhydrous cement particles with contacting water easily. And consequently, the hydration rate is accelerated in the cement after grinding.

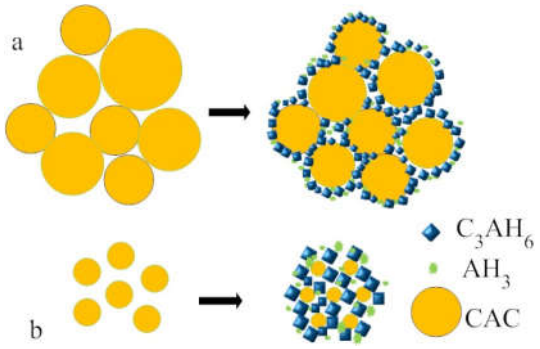

Fig. 6: Schematic representation of the hydration products of pastes of CAC (a) and mixtures (b).

CONCLUSIONS

The hydration rate of the cement paste increases with the reducing particle size of the cement at 40 °C only within a short period time (3.5h). However, there is no noticeable difference in the quantity of C_3AH_6 between the as-received and ground CAC after a long period of hydration (6h). Moreover, the degree of crystallinity of C_3AH_6 increases with the reducing particle size of CAC after hydration at 40 °C. It is probably because that the cubic C_3AH_6 forms freely during hydration in the pores of the loosely accumulated CAC particles after grinding.

ACKNOWLEDGEMENTS

The authors would like to thank the National Natural Science Foundation of China (51572244, 51372230, 51672255, 51402089, U1604252) for the financial support.

REFERENCES

[1] Ewais E, Khalil N, Amin M, Ahmed Y, Barakat M. Utilization of aluminum sludge and aluminum slag (dross) for the manufacture of calcium aluminate cement. Ceram Int. 2009;35(8):3381-8.

[2] Wang A, Zhang C, Zhang N. The theoretic analysis of the influence of the particle size distribution of cement system on the property of cement. Cem Concr Res. 1999;29(11):1721-6.

[3] Guan B, Ye Q, Wu Z, Lou W, Yang L. Analysis of the relationship between particle size distribution of α-calcium sulfate hemihydrate and compressive strength of set plaster—using grey model. Powder Technol. 2010;200(3):136-43.

[4] Bushnell-Watson SM, Sharp JH. Further studies of the effect of temperature upon the setting behaviour of refractory calcium aluminate cements. Cem Concr Res. 1990;20(4):623-5.

[5] Luz AP, Braulio MAL, Pandolfelli VC. Refractory castable engineering. FIRE Compendium Series. Germany: Göller Verlag; 2015.

[6] Bushnell-Watson SM, Sharp JH. On the cause of the anomalous setting behaviour with respect to temperature of calcium aluminate cements. Cem Concr Res. 1990;20(5):677-86.

[7] Oliveira IR, Pandolfelli VC. Castable matrix, additives and their role on hydraulic binder hydration. Ceram Int. 2009;35(4):1453-60.

[8] Zhang C, Wang Y, Guo B, Shang X, Wang Q, Ye G. Effect of Particle Size Distribution on the Hydration Behavior of Calcium Aluminate Cements. Refractories Worldforum. 2016;8 (1):75-8.

[9] Rashid S, Turrillas X. Hydration kinetics of $CaAl_2O_4$ using synchrotron energy-dispersive diffraction. Thermochim Acta. 1997;302(1):25-34.

[10] Rashid S, Barnes P, Bensted J, Turrillas X. Conversion of calcium aluminate cement hydrates re-examined with synchrotron energy-dispersive diffraction. J Mater Sci Lett. 1994;13(17):1232-4.